SANDIA REPORT
SAND2010-1371
Unlimited Release
Printed March 2010

Silicon Bulk Micromachined Hybrid Dimensional Artifact

Meghan Shilling, Hy D. Tran, Andre A. Claudet, Andrew D. Oliver, Todd M. Bauer

Prepared by
Sandia National Laboratories
Albuquerque, New Mexico 87185 and Livermore, California 94550

Sandia is a multiprogram laboratory operated by Sandia Corporation,
a Lockheed Martin Company, for the United States Department of Energy's
National Nuclear Security Administration under Contract DE-AC04-94AL85000.

Issued by Sandia National Laboratories, operated for the United States Department of Energy by Sandia Corporation.

Available to DOE and DOE contractors from
U.S. Department of Energy
Office of Scientific and Technical Information
P.O. Box 62
Oak Ridge, TN 37831

Telephone: (865) 576-8401
Facsimile: (865) 576-5728
E-Mail: reports@adonis.osti.gov
Online ordering: http://www.osti.gov/bridge

Available to the public from
U.S. Department of Commerce
National Technical Information Service
5285 Port Royal Rd.
Springfield, VA 22161

Telephone: (800) 553-6847
Facsimile: (703) 605-6900
E-Mail: orders@ntis.fedworld.gov
Online order: http://www.ntis.gov/help/ordermethods.asp?loc=7-4-0#online

SAND2010-1371
Unlimited Release
Printed March 2010

Silicon Bulk Micromachined Hybrid Dimensional Artifact

Meghan Shilling, Hy D. Tran
Primary Standards Laboratory

Andre A. Claudet
Engineering Design and Integration

Andrew D. Oliver, Todd M. Bauer
Microsystems and Components

Sandia National Laboratories
P.O. Box 5800
Albuquerque, New Mexico 87185-MS0665

Abstract

A mesoscale dimensional artifact based on silicon bulk micromachining fabrication has been developed and manufactured with the intention of evaluating the artifact both on a high precision coordinate measuring machine (CMM) and video-probe based measuring systems. This hybrid artifact has features that can be located by both a touch probe and a video probe system with a k=2 uncertainty of 0.4 μm, more than twice as good as a glass reference artifact. We also present evidence that this uncertainty could be lowered to as little as 50 nm (k=2).

While video-probe based systems are commonly used to inspect mesoscale mechanical components, a video-probe system's certified accuracy is generally much worse than its repeatability. To solve this problem, an artifact has been developed which can be calibrated using a commercially available high-accuracy tactile system and then be used to calibrate typical production vision-based measurement systems. This allows for error mapping to a higher degree of accuracy than is possible with a glass reference artifact.

Details of the designed features and manufacturing process of the hybrid dimensional artifact are given and a comparison of the designed features to the measured features of the manufactured artifact is presented and discussed. Measurement results from vision and touch probe systems are compared and evaluated to determine the capability of the manufactured artifact to serve as a calibration tool for video-probe systems. An uncertainty analysis for calibration of the artifact using a CMM is presented.

ACKNOWLEDGMENTS

The authors would like to thank the MESAFab at Sandia, John Stoup and Ted Doiron at the National Institute of Standards and Technology, and the Honeywell FM&T Kansas City Plant, especially Roger Burton and Harlan Gant, for their assistance. This work is a product of the Laboratory Directed Research and Development program at Sandia National Laboratories.

CONTENTS

Introduction 8
Artifact Design 11
Artifact Fabrication 13
Measurements 15
Evaluation of CMM Data 15
Evaluation of Edge Sharpness 18
Comparison between CMM and Video System 19
Uncertainty of Artifact Calibration 23
Methodology 23
Sources of Uncertainty 23
Results 24
Uncertainty Analysis Conclusions 25
Conclusions 27
References 29
Distribution 31

FIGURES

Figure 1: Detail of an escapement wheel from a Rolex watch. The inset is a scanning electron micrograph of the escapement. The scale bar on the SEM is 50 μm. From 8
Figure 2: Bulk micromachined step length/pitch artifact with reference surfaces. 12
Figure 3: Photograph of a macroscopic step bar; the pitch between flats is 30mm. 12
Figure 4: Artifact, design 1. 14
Figure 5: Potential artifact for micro-CMM calibration. 14
Figure 6: Point locations for CMM evaluations. 15
Figure 7: Point-by-point top surface errors from best-fit plane. 16
Figure 8: Point-by-point south sidewall errors from best-fit plane 17
Figure 9: Angle between sidewall normal and top normal 18
Figure 10: Edge measurement using fiber probe. 19
Figure 11: Example of intersection line for two planes. 20
Figure 12: Measurement by video system of a very shallow pit. 20
Figure 13: Edge distance values. 21
Figure 14: 5000 resulting intersection line cross-sections at ends and center of intersection lines. 25
Figure 15: 1σ Uncertainty along intersection line. 25

INTRODUCTION

In recent years there has been a significant increase in the number of manufacturing methods able to produce mesoscale parts with microscale features. Parts produced by these processes are found in a variety of devices, including watch components (see Figure 1), the small mirrors used in digital projection displays and ink jet heads for printers. The processes used to make mesoscale components span a wide range of fields, from traditional manufacturing such as turning and milling to lithography methods and layer-based manufacturing methods.

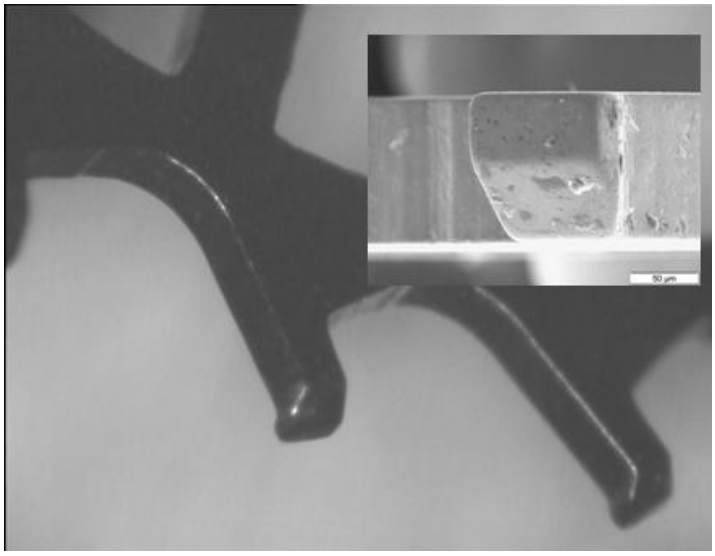

Figure 1: Detail of an escapement wheel from a Rolex watch. The inset is a scanning electron micrograph of the escapement. The scale bar on the SEM is 50 μm. From [1].

Mesoscale mechanical components are on the order of 10^0 mm in scale with features on the order of 10^{-1} mm and tolerances from 10^{-3} mm to 10^{-4} mm. Inspection of these components can be quite difficult due to lack of appropriate measurement tools. Frequently, vision-based inspection equipment is used to measure these components. These types of machines generally have a workspace greater than 100 mm × 100 mm horizontally with a lateral repeatability typically on the order of 10^{-4} mm. The most typical usage of vision based inspection equipment is inspection of parts that have 2-D characteristics. Another driver for vision-based inspection equipment is the relatively high measurement throughput. The non-contact aspect of vision based measurement is also attractive because even low contact forces can deform many mesoscale components.

An alternative to vision-based inspection, especially with parts that have requirements for features in three dimensions, is the use of micro coordinate measuring machines (micro CMMs) [2]. Micro CMMs are CMMs designed with relatively small work volumes (on the order of 100 mm × 100 mm × 100 mm), typically with touch probe stylus tips smaller than 500μm. Hybrid measurement systems are also available that combine a vision or video probe system with a touch probe system on the same machine.

Calibration of these systems is important. In vision systems, the optics and the stage are calibrated independently using different calibration artifacts. Because the artifacts used for optics

calibration contribute very little to the overall uncertainty of the system, we focused our attention on decreasing the uncertainty in the stage calibration. For commercial vision-based inspection equipment, the typical stage calibration process uses a glass reference artifact (commonly called a grid plate), with chrome cross-hairs. The uncertainty of these calibration artifacts is often the most significant component of measurement uncertainty of vision-based equipment [3] [4] [5]. Additionally, these artifacts are virtually flat, and thus not useful for tactile or hybrid measurement systems.

For tactile systems, one may follow the guidance of ASME/ANSI and ISO standards for evaluation of CMMs [6] [7]. These standards for evaluation and performance testing require the use of calibrated length artifacts. Typically, gauge blocks or step gauges are used for many of the evaluations. Unfortunately, gauge blocks and step gauges are not suited for use in vision-based systems.

To solve the problem of calibrating a vision-based system with higher accuracy than is available using a glass reference artifact, an artifact has been developed which can be calibrated using a commercially available high-accuracy tactile system and then be used to calibrate typical production vision-based measurement systems. This allows for error mapping to a high degree of accuracy, thus improving the accuracy of vision-based measurement equipment used in production.

This new artifact must have highly accurate structures that can be measured using both tactile and vision probes. The design of the artifact must take into consideration the measurement strengths and weaknesses of both systems as well as provide a straightforward methodology for both calibration by tactile probe and use on a vision system. This paper covers the design and fabrication of the artifact, CMM measurements taken using the artifact, an uncertainty analysis using a Monte Carlo simulation, and methods of improving the artifact.

ARTIFACT DESIGN

The primary design objective for the calibration artifact is to have features that accommodate both vision and touch probing. Vision systems are very good at detecting sharp edges, so the geometric features inspected by the touch probe must also be able to be reduced to edges (e.g., intersection of two planes to construct a straight edge). Bulk silicon micromachining was chosen for manufacture of this artifact due to some very convenient properties, which will be explained in more detail.

Bulk silicon micromachining has a long history. Recent work, which varies processing parameters, using different wet etch conditions, mask optimization, and different masks and etch stops, has greatly increased the possible geometries producible with bulk micromachining. Commercial applications of this technology include pressure sensors and automotive airbag accelerometers.

A useful result of silicon bulk micromachining is that the angles created by anisotropic etching are defined intrinsically by the crystalline structure of the silicon. By use of single crystal material, we can ensure that all of the crystal planes are parallel. Silicon of all crystal orientations, when etched in an anisotropic etchant, such as potassium hydroxide (KOH), etches 400 times faster in the <100> direction than in the <111> direction [8]. This anisotropic etching has the capability to produce exposed crystal planes that are smooth within a few nanometers. Published results vary from a roughness rms of a few nm for a small area [9] to a peak-to valley value of several μm [10]. Variations in roughness appear to be attributable to both the process used as well as the size of the measured area.

Anisotropically etched <100> silicon has sidewalls that are angled at 54.74 degrees ($\cos^{-1}\left(\frac{1}{\sqrt{3}}\right)$) from vertical due to the orientation of the crystal structure, which is reproducible for all structures on the same wafer. As a result of the gentle slope, the silicon wafer does not have to be especially thick (1.5 mm is adequate) in order to define a plane with the touch probe. However, the bottom of an etched cavity is not necessarily flat, limiting the use of the bottom as a calibration surface.

In addition to providing good geometry, silicon has desirable properties as a mechanical material including high purity (part-per-million to part-per-billion level), high mechanical fracture strength (>0.6 GPa), and high Young's modulus (165 GPa). Also, because silicon is a brittle material, it will break rather than yield [11]. The material properties (CTE, etc.) are well studied for silicon due to the semiconductor industry.

The silicon bulk micromachining process creates sidewalls that form a sharp and straight intersection line with the top surface of the wafer. This intersection line can be measured by both a touch probe and a vision probe. The touch probe reconstructs the line by intersecting the measured top and etched sidewall plane. The vision probe measures the intersection line directly. The same features that are measured with the touch system are also measurable by a vision system, thus creating a "hybrid artifact". The design of the artifact (the arrangement of the lines)

is critical to its success, especially when considering the characteristics of vision measurement systems.

Illumination of an object under measurement by a video probe is extremely important to the validity of the end result [12]. Both the type of illumination and the illumination level need to be chosen when measuring with a video system. Type of illumination is usually dictated by the object being measured, but the level of illumination is operator-selected from within an accepted range. Changing the illumination level, even within the accepted range, can change the measured size of an object, but the centroid of the object is rarely affected. As a result, an etched pit may grow and shrink in size with illumination changes. The centroid, however, will not move. If we measure the pitch between pits, the result should be unaffected by illumination level.

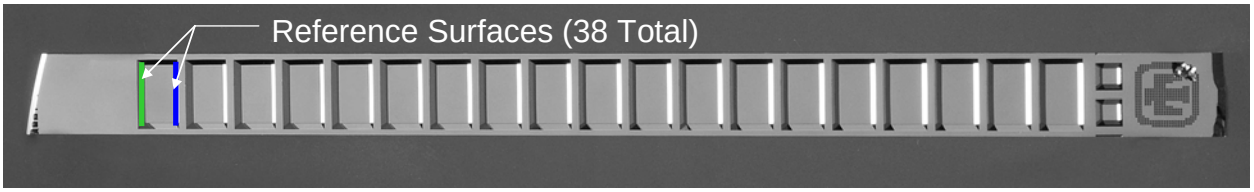

Figure 2: Bulk micromachined step length/pitch artifact with reference surfaces.

Thus, our artifact contains series of well-defined lines, created by etching pits into the silicon. The artifact can be calibrated with a vision system and subsequently used to calibrate the lateral (x-y) dimensions of a vision-based measurement system. The series of pits, show in Figure 2, is similar to a step bar, pictured in Figure 3, but instead of measuring the distance between planes, the distance between edges is measured. Comparison between the calibration by the touch probe system (high accuracy) and the measurement by a video probe (high resolution, current accuracy approximately 10x worse than resolution) allows for error mapping of the video measurement system by use of standard algorithms.

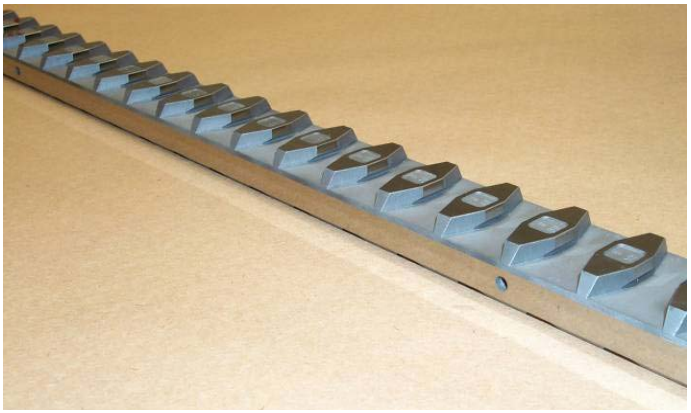

Figure 3: Photograph of a macroscopic step bar; the pitch between flats is 30mm.

ARTIFACT FABRICATION

Process development for the manufacturing of the artifact using bulk silicon micromachining, was undertaken by the MESAFab group at Sandia. The process development goal was to determine the processing parameters that would minimize surface roughness of the sidewalls. Design of experiments was implemented to determine the optimal process parameters, varying rinse agent and etchant (including chemistry, concentration, and temperature). Both IPA (Isopropyl Alcohol) and water were considered as rinse agents. Potassium hydroxide (KOH), ammonium hydroxide (NH3), and tetramethyl ammonium hydroxide (TMAH) were tested as etchants, at various concentrations and temperatures. Details can be found in [12].

The roughness was measured by atomic force microscope (AFM). Although roughness on the sidewalls is of particular importance to this project, the AFM was unable to measure the sloping surface, instead measuring the bottom of the trenches. We hope that by minimizing the surface roughness of the bottoms of the trenches, we have also minimized the surface roughness of the sidewalls. The AFM measured both a small area (5 x 5 μm) and a large area (30 x 30 mm).

Nineteen trials were run with various processing parameters. Based on the results, final processing parameters were chosen to optimize the combination of surface smoothness, etch rate, and selectivity. KOH at a concentration of 6M and temperature of 80 ºC was selected as the etchant for its combination of smoothness, etch rate, and selectivity. The total time to etch 1 mm, the etch depth for all designs, is about 17 hours.

Two different artifact designs were fabricated using 1.5 mm thick, 150 mm diameter single crystal <100> silicon. The first design has a series of step structures that can be separated into 13 individual artifacts (see Figure 2). This artifact, as produced, is shown in Figure 4. The second design contains a variety of experimental structures, including pits for holding arrays of spheres. The center square section of the artifact is 100 x 100 mm and is intended to be separated from the remaining structures and mounted on glass, as shown in Figure 5. We are investigating the use of this section as a micro-CMM calibration artifact.

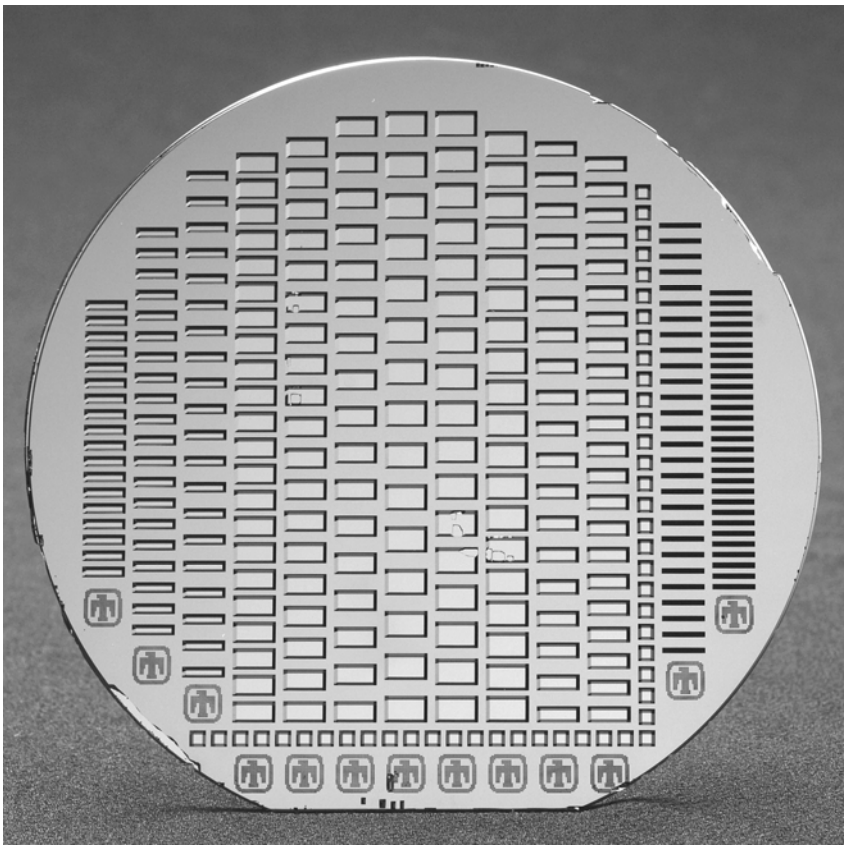

Figure 4: Artifact, design 1.

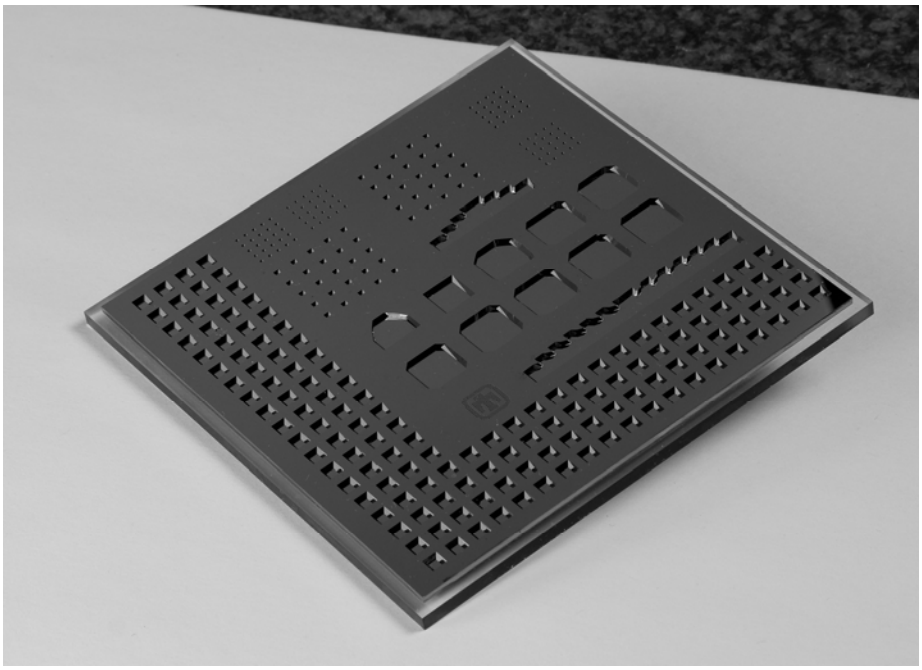

Figure 5: Potential artifact for micro-CMM calibration.

MEASUREMENTS

A number of important characteristics of the produced artifacts have been evaluated using a variety of measurement systems. A Leitz PMM-C Infinity CMM has been used to collect nominal surface points for a number of different evaluations. This system is located in the Primary Standards Laboratory at Sandia National Laboratories. It has single-axis repeatability of approximately 50 nm (k=2) and a volumetric performance of (0.3 + L/1000) μm, where L is the distance measured in mm. This CMM is capable of being used to calibrate the silicon artifacts to be used on a vision system.

A Mitutoyo UMAP optical fiber-probe system at the National Institute of Standards and Technology was used to determine the sharpness of the produced edge. The accuracy of the system is (1.2 + L/300) μm with repeatability better than 0.1 μm.

An OGP Smartscope Apex vision system, housed in the Mechanical Calibrations Laboratory at Sandia National Laboratories, was used to evaluate the relevant properties of the silicon artifact as well as in comparison with the CMM data. This system has resolution of 0.1 μm with an accuracy of ±3 μm.

Evaluation of CMM Data

A CMM was used to collect data from the dimensional artifact. The hybrid dimensional artifact, as shown in Figure 5, has several rows of square pit features. A line of 19 3 mm × 3 mm squares was measured. Twenty-four points from around the top surface of each square (6 points in each of four locations) and 16 points on each of two opposite sidewalls (North and South) were collected for all of the 19 squares (see Figure 6). These points are used both to evaluate the geometry and surface quality of the produced artifact as well as to establish the location of the edge for comparisons to vision system measurements.

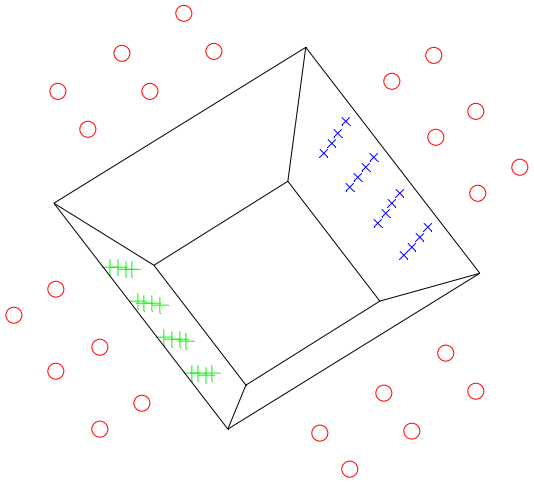

Figure 6: Point locations for CMM evaluations.

The intersection line between the sidewall and the top surface is calculated independently for the North and South sidewalls. Given data points lying on the two distinct planes, the best-fit plane for each surface is found and the intersection line of the two best-fit planes is calculated. The planes are fit using a highly accurate least-squares reference algorithm specified by Shakarji [13]. The algorithm uses Lagrange multipliers on a constrained minimization problem. Resulting from this algorithm is a point that lies on the plane and a normal vector for each of the fit planes. The line of intersection is calculated directly from these quantities using widely available analytic equations.

The measurements were evaluated for their deviations from the best fit top and sidewall planes and the angle between the normal vectors of the best fit top and sidewall planes. Results comparing the location of the edge to that found using a video system are presented in a later section.

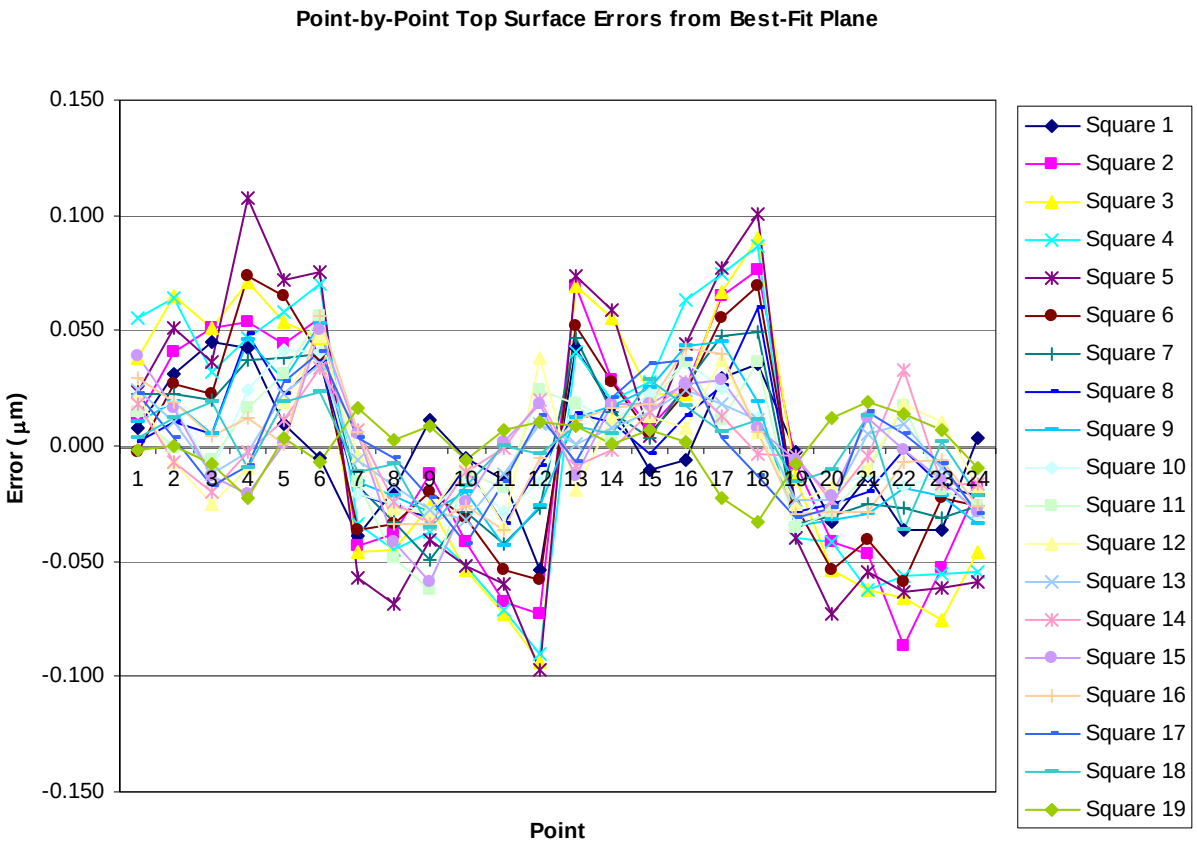

Figure 7: Point-by-point top surface errors from best-fit plane.

Data from the top surface of the artifact is shown in Figure 7. Six data points were taken in each of four areas. It is possible to distinguish these four areas in the figure. The variability in this data comes from three sources: the CMM repeatability, the roughness of the surface, and the flatness of the top surface. Based on this figure, as well as other collected data, the peak-to-valley roughness of the surface is estimated to be approximately 50 nm and the peak-to-valley flatness

as 100 nm over 5 mm. These numbers are used in the uncertainty analysis calculations. These numbers are on the order of what was expected based on manufacturers claims and previous experience.

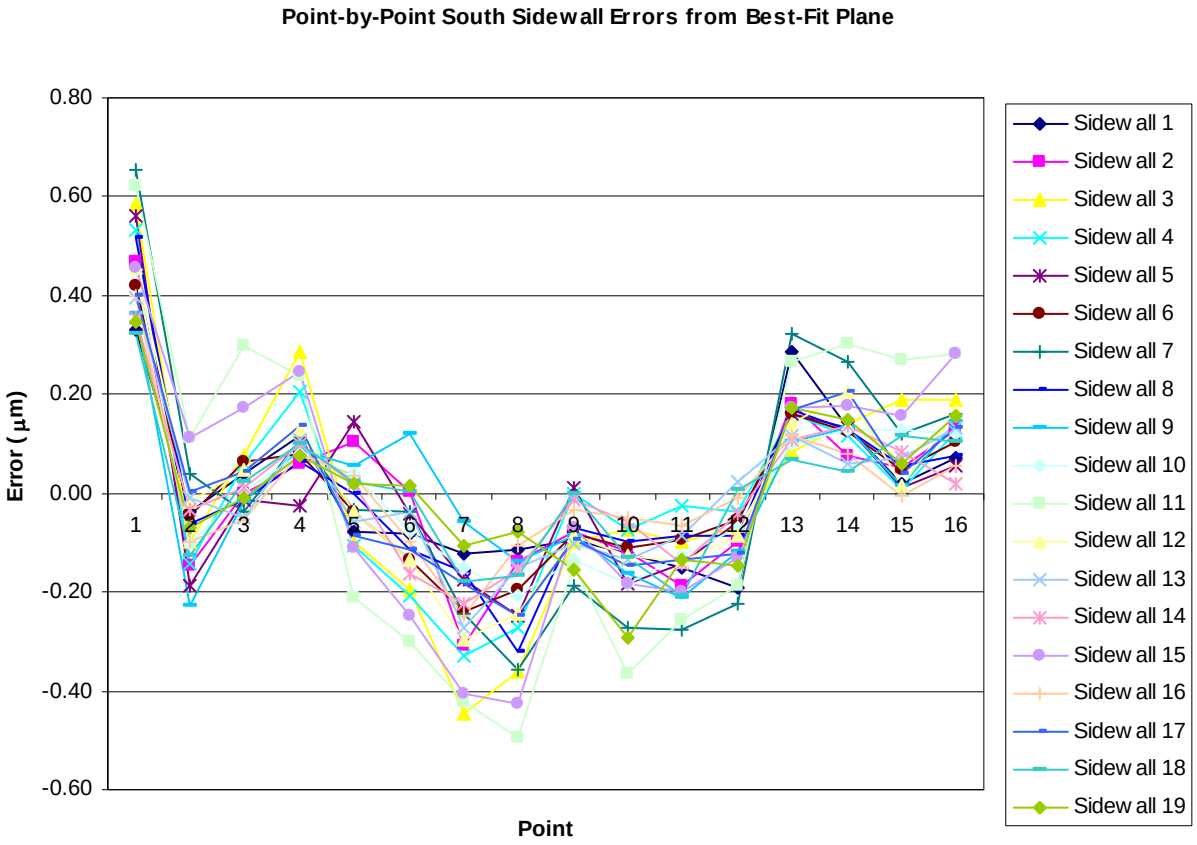

Figure 8: Point-by-point south sidewall errors from best-fit plane.

Data from the south sidewall of the artifact is shown in Figure 8. Data from the north sidewall has a similar appearance. Sixteen data points were taken in four rows of four. The variability in this data comes from the CMM repeatability and the roughness of the surface. Based on this figure, as well knowledge of the CMM and other collected data, the combination of roughness and flatness for the sidewalls is estimated to be approximately ±0.6 µm. These numbers are used in the uncertainty analysis calculations.

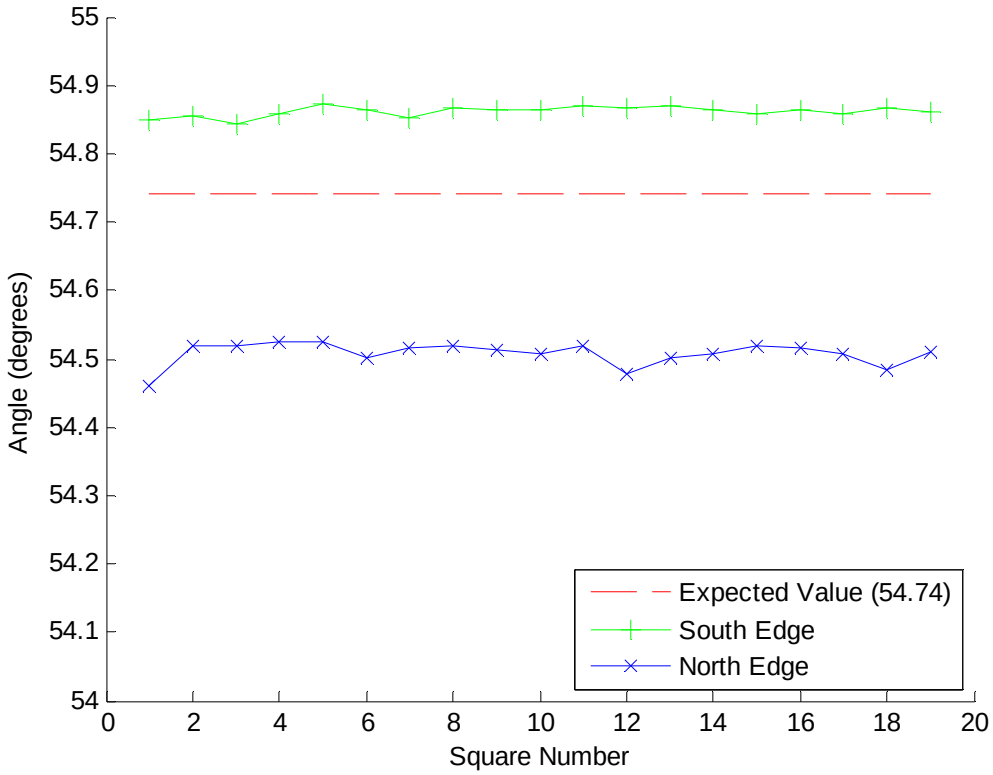

Figure 9: Angle between sidewall normal and top normal

When anisotropically etched, the bulk silicon used to produce the artifact should have sidewalls that are angled at 54.74 degrees from vertical due to the orientation of the crystal structure. A slight misalignment of the crystal structure to the top surface of the wafer would have an effect on the angle between the sidewall normal and the top plane normal. Because we are evaluating sidewalls that are on opposite sides of the crystal structure, a misalignment error would make one angle higher while making the other lower. This is in fact what we observe from the CMM measurements. Figure 9 shows the angle between the sidewall normal and top plane normal for each of the 19 squares, both the north and south edges. The angle at the south edge is higher than expected, with a mean of 54.86 degrees, and range of 0.03 degrees. The angle at the north edge is lower than expected, with a mean of 54.51 degrees and range of 0.06 degrees. The misalignment of the crystal structure with the top plane does not affect the parallelism of the etched reference surfaces.

Evaluation of Edge Sharpness

In addition to the characteristics of the surfaces as measured by the CMM, the sharpness of the edge between the sidewall is also critical, because it is being used by the video probe as a calibration feature. In order to map the imaged edge with that edge calculated from CMM measurements, it is necessary that the edge be a perfectly sharp intersection of two planes.

The optical fiber-probe system described above was used to determine the sharpness of the edge. This system uses a 2 mm long fiber with a 30 μm diameter ball on the end. The probe vibrates at

a known frequency. As it comes in contact with an object, the frequency of vibration changes and a measurement point is taken.

Five traces were taken over the edge of a step object on the artifact. The traces are shown in Figure 10. In this figure, the trace represents the probe center location as it traces over the edge of the object. When a round object traces over a sharp edge, the location of the center of the round object is influenced by its diameter, and the resulting trace should have a radius that is the same as that of the round object. It can be see in Figure 10, that the trace correlates nicely to the shape of the probe. This indicates that the edge of the artifact is quite sharp. The small deviations from the probe shape are most likely attributable to imperfections in the probe (the ball is not perfectly spherical).

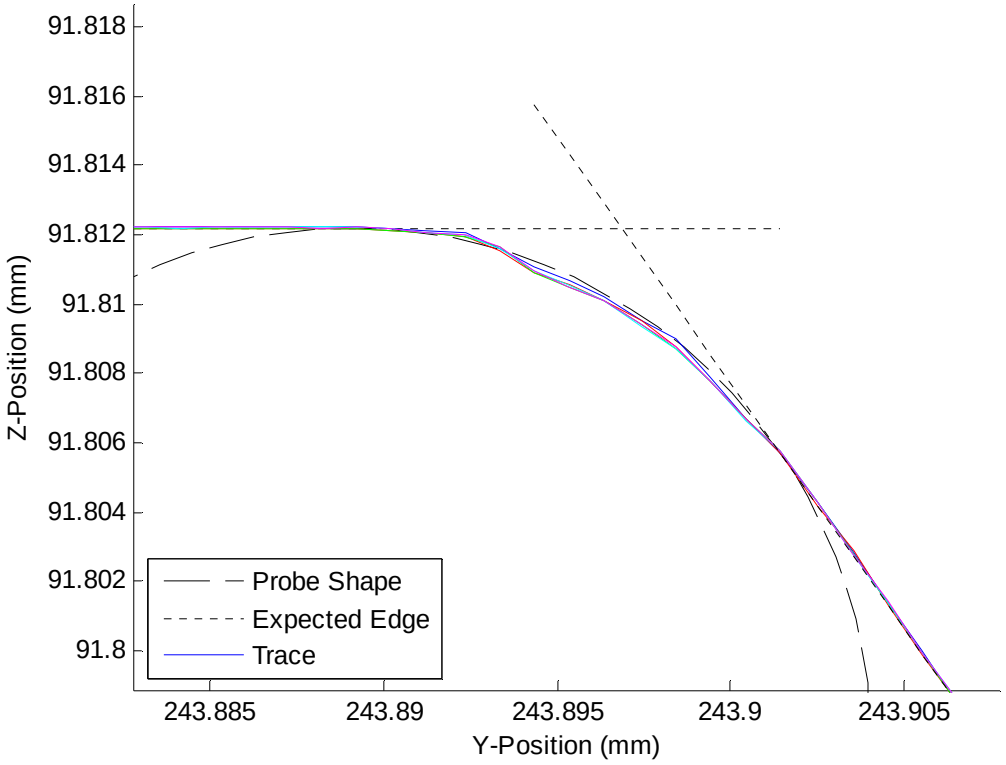

Figure 10: Edge measurement using fiber probe.

Comparison between CMM and Video System

To show the feasibility of this object as a calibration artifact, measurements taken with a CMM and two video systems were compared. The high accuracy CMM was used to probe both the sidewalls and the top surface of the artifact. Assuming perfect geometry, the computed intersection of the planes is the edge between the two, which can be imaged with a vision-based inspection system using coaxial lighting.

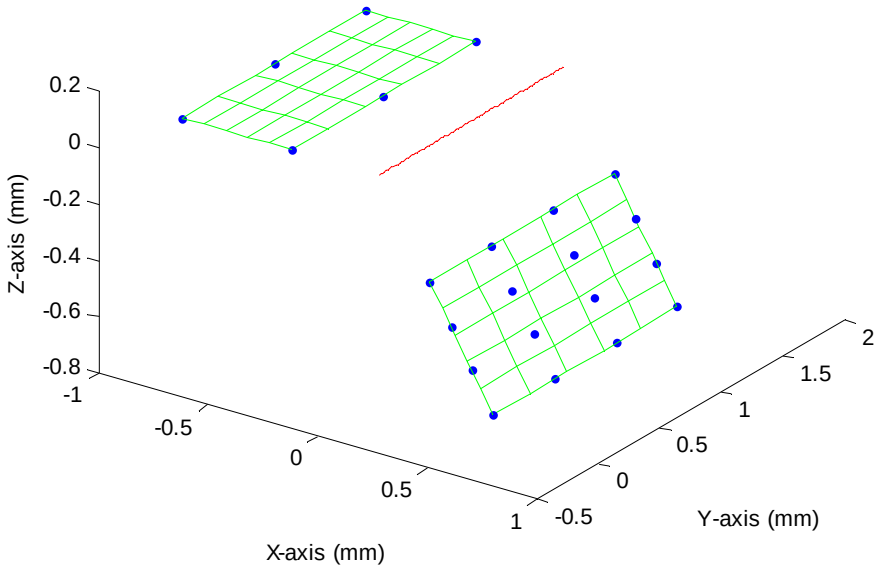

Figure 11: Example of intersection line for two planes.

The coordinate measurement machine locates an edge line by finding the intersection of the top plane and the sidewall, as shown in Figure 11. In this test, 24 points are measured on each the top surface, 16 on each sidewall. The two planes are found using a least-squares fitting routine, and the edge line calculated by intersection of these two planes. This process is repeated for 19 edge areas and the pitch calculated for consecutive line pairs.

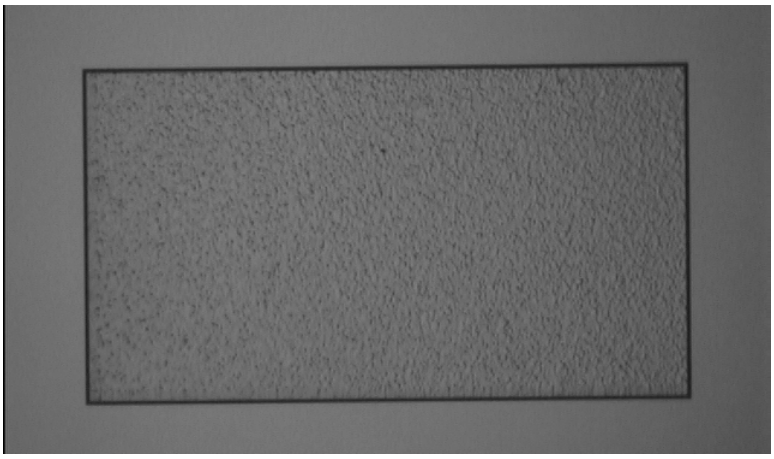

Figure 12: Measurement by video system of a very shallow pit.

The video system locates the same edges through use of internal edge detection and line fitting software. Each line is located and the pitch determined for each line pair. An example of a very shallow pit as seen by a video system is shown in Figure 12. Note the roughness of the bottom of the pit and the black band around the perimeter that is the etched sidewalls. The combination of steepness and smoothness in the sidewall yields sharp contrast between the top surface and the sidewall, which results in good edge location.

Repeatability and invariability under different lighting conditions have been tested on multiple video systems [14]. The video systems have been tested at a range of lighting intensities, representing both the nominal operating intensity as well as intensities above and below the suggested working range. The video measurement systems showed a high degree of repeatability under varying light intensities. It was observed that the lines shift slightly under changing lighting condition, but it appears that all lines shifted by the same amount, resulting in a stable pitch with respect to light intensity.

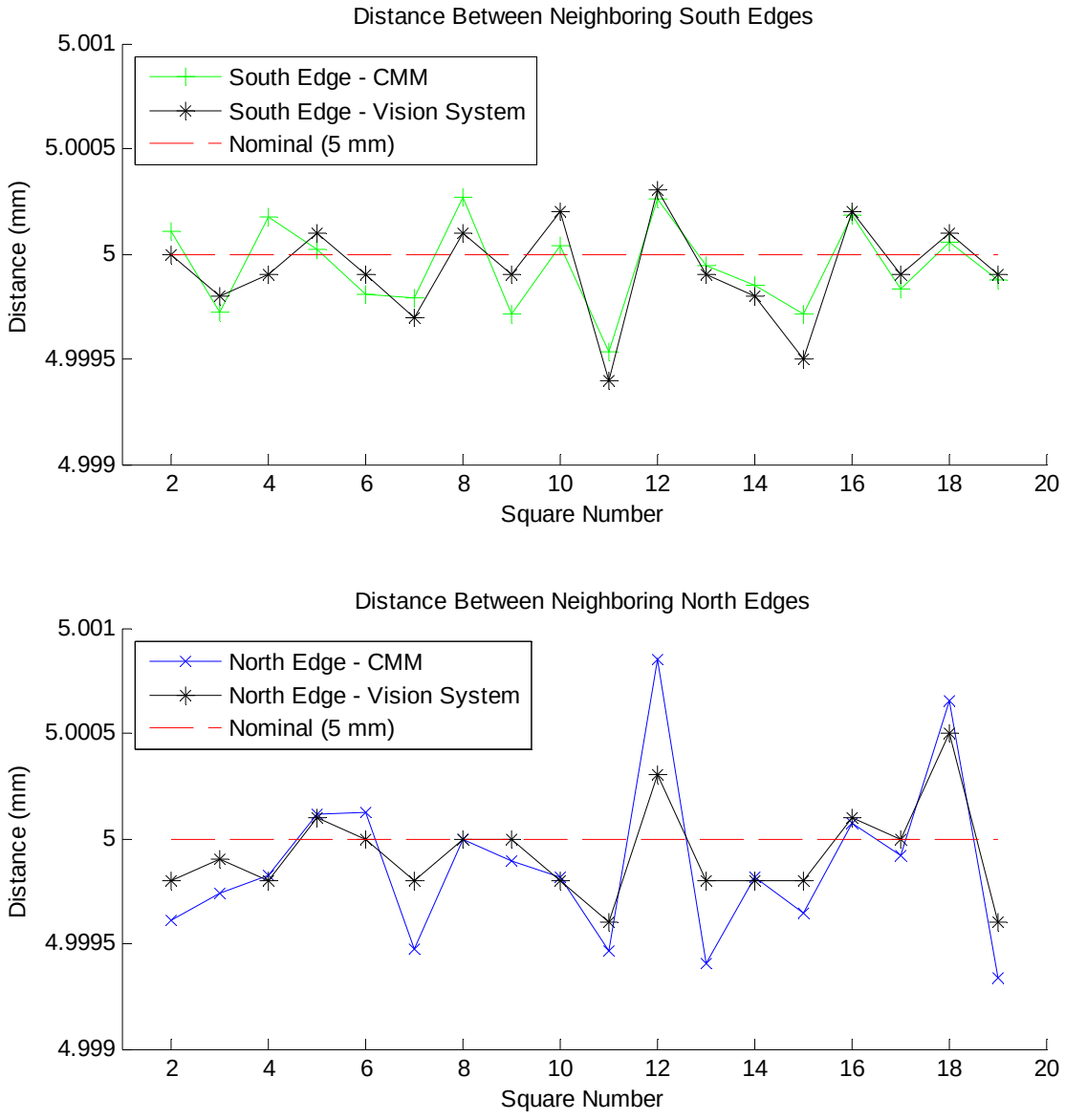

Figure 13: Edge distance values.

Figure 13 is a comparison of the edge distance values from the CMM and vision system. Looking at the south edges, the average difference between the CMM and the vision system measurements is 100 nm, with a maximum of 270 nm. For the north edges, the average difference is 140 nm with a maximum of 550 nm. These differences are well within the uncertainty of the vision system.

UNCERTAINTY OF ARTIFACT CALIBRATION

To determine the feasibility of using silicon bulk micromachining to create a calibration artifact, it is important to understand the uncertainty present in the touch-probe measurements. The most critical feature is the distance between lines created by the intersection of the sidewall and the top plane. The touch-probe does not measure these lines directly, but instead calculates it based on the intersection between two best-fit planes. The uncertainty in the calculated line is important because the positions of the intersection lines calculated from data collected on the CMM will be compared to the line directly measured by the video-probe system. In order to provide an improved calibration artifact, we would like the uncertainty of line location to be less than 100 nm, an order of magnitude lower than uncertainty of current calibration artifacts.

Methodology

The uncertainty of a single line location was calculated using a Monte Carlo Simulation, with knowledge of expected uncertainty due to CMM repeatability, sidewall flatness and roughness, and top surface flatness and roughness. Additional details are presented in [4].

The standard method for uncertainty evaluation is described in the U.S. Guide to the Expression of Uncertainty in Measurement (GUM) [15]. Unfortunately, due to the complexity of the intersection line calculation, using the GUM methodology to determine the associated uncertainty is exceedingly complicated because sensitivity coefficients can not be derived analytically [16]. An alternative to this calculation is to use a Monte Carlo simulation to estimate the uncertainty. Monte Carlo simulations estimate the uncertainty in a measurement by assessing the uncertainty present in a large number of trials whose input conditions are varied according to the expected magnitude and distribution of uncertainty sources.

Monte Carlo simulation has been used by Schwenke et al. [16], Cox et al. [17], Trapet et al. [18], Balsamo et al. [19] and others to assess measurement uncertainty. In addition, the 2008 GUM includes a supplemental guide that deals with the use of Monte Carlo simulation as a tool for evaluating measurement uncertainty through the propagation of distributions [20].

To determine the uncertainty using a Monte Carlo simulation, it is necessary to first understand the individual sources of uncertainty which contribute to the overall uncertainty of the measurement, and their respective probability distribution functions (PDF). Once these sources are identified, a model is built to mimic the process which calculates the quantity of interest. In this case the model is dictated by the methods used to calculate each of the best-fit planes and the line formed by their intersection.

Sources of Uncertainty

For this work, the uncertainty lies in the measurement points. Measurement point uncertainty comes from two sources – the touch-probe and the imperfect surface of the part.

High accuracy CMMs are available, with volumetric performance of (0.3 + L/1000) μm and repeatability in a single axis below 100 nm. Highly specialized CMMs in extremely well controlled environments are capable of achieving even lower single axis repeatability. The touch-probe uncertainties used here are modeled based on the repeatability values for each axis

of very high accuracy CMM over a limited span of time. The calculations assume one-sigma repeatability values, based on observation, of 25 nm for the two horizontal axes, and 15 nm for the vertical axis. A Gaussian distribution is used to model these uncertainties.

The ball on the end of the stylus, which contacts the surfaces of the artifact, has uncertainty associated with it- the size is typically not known to the nm level, and the ball is not perfectly round. However, we can neglect these two sources of uncertainty because they cause a bias which is constant over all lines measured in a single direction. Therefore the uni-directional distance between lines, which is what we are calibrating, is not affected.

Uncertainty due to surface imperfections is a result of the combination of surface roughness and surface planarity. These numbers are taken from observations of CMM data presented earlier. Peak-to-valley surface roughness of the top plane is approximately ±50 nm with surface planarity of 50 nm over 5 mm. For the sidewall, the combination of surface roughness and planarity observed was approximately ±0.6 μm. The uncertainty values due to surface imperfections are modeled as uniform rectangular distributions.

With an understanding of magnitude and sources of point uncertainty and a mathematical model, a Monte Carlo simulation can be run. Each test case starts with the intended measurement points and adds a randomized variation based to the point uncertainty model to create simulated measured data points. The simulated data points are evaluated to determine an intersection line using the algorithm described above. A large number of test cases are run and the set of all intersection lines from the test cases is evaluated to estimate the uncertainty of the intersection line under the given conditions.

Results

The results presented in Figure 14 are from a Monte Carlo trial based on the expected touch-probe measurement locations and associated point uncertainties. Monte Carlo trials were run with up to 250,000 data sets. Figure 14 shows x-z cross sections of the set of lines at the ends and center of the measurement area for a smaller trial of 5000 data sets. The uncertainty region appears elliptical and varies slightly in size by position along the intersection, with the smallest variation in the center of the measurement area.

In order to quantify the uncertainty, the standard deviations (σ) along the major and minor axes of the elliptical region are calculated. An improved algorithm is used to determine the major axis, as standard routines assume no uncertainty in the abscissa.

The 1σ values at different points along the fit line are given in Figure 15. As expected based on the pattern seen in Figure 14, the deviations are slightly higher at the ends of the line than in the middle. The k=1 uncertainty, or 1σ value, along the major axis is approximately 0.21 μm at the ends, and 0.19 μm in the center of the measurement area. The uncertainty along the minor axis is approximately 0.02 μm.

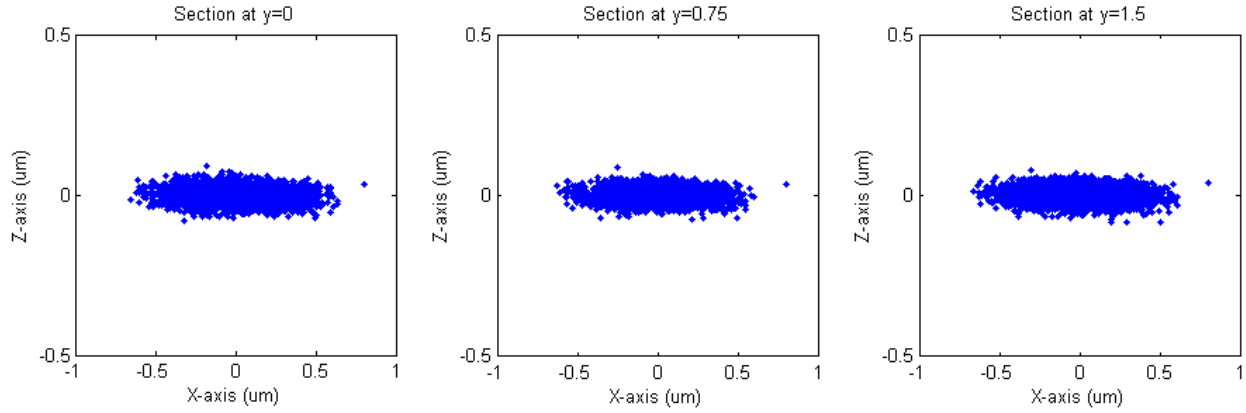

Figure 14: 5000 resulting intersection line cross-sections at ends and center of intersection lines.

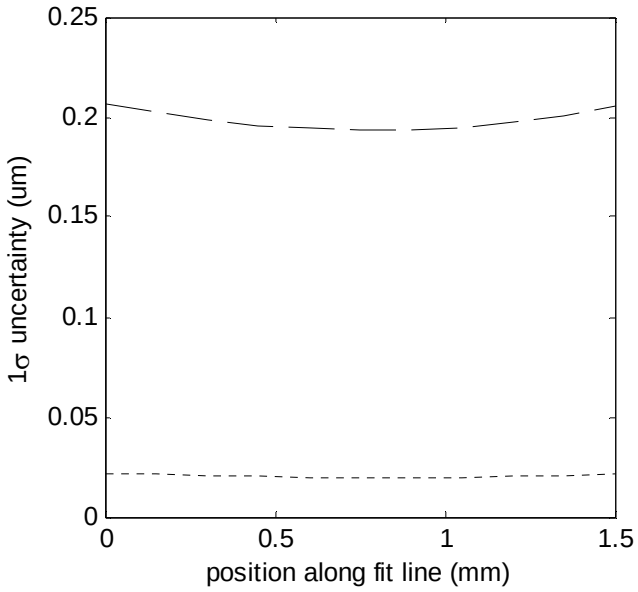

Figure 15: 1σ Uncertainty along intersection line.

Tests were also run which used a sidewall surface uncertainty which is achievable, according to previous experimental work, but lower than that of our produced artifacts. This test showed that if the uncertainty due to sidewall surface texture can be minimized by process optimization to a level of ±50 nm, it is possible to achieve a k=1 uncertainty in line location of 25 nm. Details on this trial and other trials can be found in [4].

Uncertainty Analysis Conclusions

Current optical calibration artifacts have uncertainty levels around 1 μm at k=2. The goal is to create an artifact that can be calibrated with a CMM with resulting uncertainty levels at 1/10 of the current value, or approximately 100 nm at k=2. Due to surface roughness on the sidewalls, the calibration artifact, as produced, has a k=2 uncertainty of approximately 0.4 μm. However,

with process optimization an uncertainty of less than 50 nm is attainable; more than 20 times better than the accuracy of current calibration artifacts.

CONCLUSIONS

This article describes an artifact designed to be used to calibrate the stage of a vision system. The innovation is in the use of a common geometry, in this case the edge formed by the intersection of two planes, which can be calibrated by CMM and measured by a vision system. Because the CMM has the ability to calibrate the artifact to a higher degree of accuracy (k=2 uncertainty of 0.4 μm for produced artifacts, potential uncertainty as low as 50 nm at k=2) than current vision calibration artifacts (k=2 uncertainty of approximately 1 μm), the overall uncertainty of vision system measurements can be decreased. The artifact is also useful for calibrating hybrid systems which use both vision and touch probing.

Silicon bulk micromachining is used to create the sharp edges of the dimensional artifact. The need for sharp edges and smooth sidewalls led to a design of experiments study, which resulted in a better understanding of the effects of processing parameters, such as mask alignment, etchant properties, and nitride removal processes, on sidewall roughness. Wafers were produced using the optimized parameters.

Based on experience, we believe that it is possible to achieve surface variations on the order of ±50 nm for an anisotropically etched silicon sidewall. However, even with process optimization, we are still an order of magnitude away from achieving this surface quality. Very little work has been done to investigate the surface quality of sidewalls, including the potential causes for roughness. Work by Merveille [21] suggests that surface imperfections may originate from mechanical stress in the wafer or precipitation of impurities, such as oxygen, during processing. We continue to work towards better sidewall surface quality.

Even with the roughness present, feasibility of the hybrid dimensional artifact has been established both by simulation and by measurement. Measurements of a step structure on the prototype artifact show agreement between the CMM and vision systems. Tests indicate the insensitivity of pitch measurements under varying lighting intensities. This repeatability is critical to the success of the dimensional artifact, as the operating light intensity is operator dependent.

The cost of these artifacts is also of great interest when considering commercialization. The incremental cost of these artifacts (not counting initial set-up and development costs) is largely driven by the cost of the raw wafer plus the cost of the labor needed to process the wafer to its final stage. In small quantities a 1.5 mm thick, 6” raw silicon wafer is $100. The largest expense for manufacturing comes from labor, not from materials, so if we consider only labor costs: cleaning and patterning requires about 2 hrs of labor per wafer, etching time is approximately 17 hrs (but at least 6 wafers can be etched at one time), dicing/sawing, and packaging adds about 1 hr of labor per wafer. Therefore, a conservative estimate is 6 hrs of labor per wafer. If the labor rate is $1/min (typical commercial rate), each wafer would cost approximately $460. Of particular interest are the step structures on the 2D wafer. Each 2D wafer yields 13 devices, so each 2D step structure would be less than $50 to manufacture. This price, however, does not include calibration. We estimate an additional 1-2 hrs of labor for calibration of the artifact.

The artifact, with its novel use of silicon micromachining to produce structures measurable by touch and vision systems, shows great potential as a new, higher-accuracy, vision calibration artifact.

REFERENCES

1. Lohr, C., and G.L. Benavides. "Lessons from the Watch Industry." Paper presented at the Sandia Student Intern Symposium, Albuquerque, New Mexico 2007.
2. Claudet, Andre A., Edwin A. Bryce, and Hy D. Tran. "Initial Evaluation of a Micro-Cmm." Paper presented at the NCSLI Workshop and Symposium, St. Paul, Minnesota 2007.
3. Mason, Shawn. "In House Capability for Calibration of an Optical Cmm for Any Company." Paper presented at the NCSLI Workshop and Symposium, St. Paul, Minnesota 2007.
4. Shilling, Meghan, Andre A. Claudet, Andrew D. Oliver, and Hy D. Tran. "Uncertainty Analysis for a Silicon Bulk Micromachined Dimensional Metrology Artifact." Paper presented at the ASPE Annual Meeting, Monterey, California 2006.
5. Oliver, Andrew D., Hy D. Tran, and Andre A. Claudet. "Design of a Silicon Micromachined Artifact for Hybrid Dimensional Measurement." Paper presented at the ASME International Conference on Manufacturing Science and Engineering, Ypslianti, Michigan 2006.
6. ASME. "Methods for Performance Evaluation of Coordinate Measuring Machines." In *B89.4.1b-2001*, 2001.
7. ISO. "Geometrical Product Specifications (Gps) - Acceptance and Reverification Tests for Coordinate Measuring Machines (Cmms)." In *10360, part 2*, 2001.
8. Petersen, K. "Silicon as a Mechanical Material." *Proceedings of the IEEE* 7, no. 5 (1982).
9. Ezoe, Yuchiro, Masaki Koshiishi, Makato Mita, Kazuhisa Mitsuda, Akio Hoshino, Yoshitaka Ishisaki, Zhen Yang, Takayuki Takano, and Ruytaro Maeda. "Micropore X-Ray Optics Using Anisotropic Wet Etching of (110) Silicon Wafers." *Applied Optics* 45, no. 35 (2006): 8932-38.
10. Strandman, Carola, Lars Rosengren, Håkan G. A. Elderstig, and Ylva Bäcklund. "Fabrication of 45º Mirrors Together with Well-Defined V-Grooves Using Wet Anisotropic Etching of Silicon." *Journal of Microelectromechanical Systems* 4, no. 4 (1995): 213-19.
11. William T. Sharpe, Jr. "Mechanical Properties of Mems Materials." In *Mems: Introduction and Fundamentals*, edited by M. Gad-el-Hak: CRC Press, 2006.
12. Tran, Hy D., Meghan Shilling, Andre A. Claudet, Andrew D. Oliver, Todd M. Bauer, Matthew G. Hankins, David L. Luck, Jonathan D. Weiss, Bernhard Jokiel, and Larry J. Azevedo. "Silicon Bulk Micromachined Hybrid Dimensional Artifact." Albuquerque, NM: Sandia National Laboratories, 2007.
13. Shakarji, C.M. "Least-Squares Fitting Algorithms of the Nist Algorithm Testing System." *Journal of Research of NIST* 103, no. 6 (1998): 633-41.
14. Shilling, Meghan, John Stoup, Theodore Doiron, Andre A. Claudet, and Hy D. Tran. "Measurement Results for a Hybrid Dimensional Artifact." Paper presented at the NCSLI Workshop and Symposium, St. Paul, Minnesota 2007.
15. ANSI/NCSL. "American National Standard for Calibration - U.S. Guide to the Expression of Uncertainty in Measurement." In *Z540-2-1997*, 1997.
16. Schewenke, H., B.R.-L. Siebert, F. Wäldele, and H. Kunzmann. "Assessment of Uncertainties in Dimensional Metrology by Monte Carlo Simulation: Proposal of a Modular and Visual Software." *Annals of the CIRP* 49 (2000): 395-98.
17. Cox, M., P. Harris, and B.R.-L. Siebert. "Evaluation of Measurement Uncertainty Based on the Propagation of Distributions Using Monte Carlo Simulation." *Measurement Techniques* 46, no. 9 (2003): 824-33.

18. Trapet, E., E. Savio, and L. De Chiffre. "New Advances in the Traceability of Cmms for Almost the Entire Range of Industrial Metrology Needs." *Annals of the CIRP* 53 (2004): 433-38.
19. Balsamo, A., M. Di Ciommo, R. Mungo, B.I. Rebaglia, E. Ricci, and R. Grella. "Evaluation of Cmm Uncertainty through Monte Carlo Simulations." *Annals of the CIRP* 48 (1999): 425-28.
20. JCGM. "Evaluation of Measurement Data - Supplement 1 to The "Guide to the Expression of Uncertainty in Measurement" - Propagation of Distributions Using a Monte Carlo Method." In *JCGM 101:2008*, 2008.
21. Merveille, Chris. "Surface Quality of {111} Side-Walls in Koh-Etched Cavities." *Sensors and Actuators A* 60 (1997): 244-48.

DISTRIBUTION

1	Andrew D. Oliver mrandrewoliver@gmail.com		(electronic copy)
2	John Stoup (john.stoup@nist.gov) Ted Doiron (Theodore.doiron@nist.gov) National Institute of Standards and Technology		(electronic copies)
1	MS0613	S. G. Barnhart	02540 (electronic copy)
1	MS0665	L. J. Azevedo	02542 (electronic copy)
1	MS0665	E. H. Detlefs	02541 (electronic copy)
1	MS0665	K. M. Shilling	02541 (electronic copy)
1	MS0665	H. D. Tran	02541 (electronic copy)
1	MS1064	A. A. Claudet	02614 (electronic copy)
1	MS1077	T. M. Bauer	01746 (electronic copy)
1	MS1451	A. J. Medina	02500 (electronic copy)
1	MS0899	Technical Library	09536 (electronic copy)
1	MS0123	D. Chavez, LDRD Office	01011 (electronic copy)
1	MS0161	Legal Technology Transfer Center	11500 (electronic copy)


Sandia National Laboratories